A ratiometric fluorescent sensor of a terbium coordination polymer for the anthrax biomarker 2,6-dipicolinic acid with on-site detection assisted by smartphone APP

Miao-Miao Qiu,[a] Ke-Fu Chen,[b] Qi-Rui Liu,[a] Wei-Ni Miao,[c] Bing Liu,[a*] and Ling Xu[c*]

[a.] College of Chemistry and Chemical Engineering, Shaanxi Key Laboratory of Chemical Additives for Industry, Shaanxi University of Science and Technology, Xi'an 710021, Shaanxi Province, P. R. China
E-mail: liubing@sust.edu.cn

[b.] College of Information Engineering, Henan University of Science and Technology, Luoyang 471000, Henan Province, P. R. China.

[c.] Key Laboratory of Macromolecular Science of Shaanxi Province, Shaanxi Key Laboratory for Advanced Energy Devices, Shaanxi Engineering Laboratory for Advanced Energy Technology, School of Chemistry & Chemical Engineering, Shaanxi Normal University, Xi'an 710062, Shaanxi Province, P. R. China

Table S1. The structural determination and refinement data for Tb-NDBC.

Empirical formula	$C_{13}H_6O_6Tb$
Color and Habit	Colorless platelet
Crystal Size (mm^3)	0.22 × 0.16 × 0.05
Crystal system	monoclinic
Space group	$P2_1/c$
a (Å)	12.9504(7)
b (Å)	12.8021(6)
c (Å)	6.8288(4)
α/°	90
β/°	94.149(5)
γ/°	90
V/Å^3	1129.20(10)
Z	4
Fw	417.10
D_{calcd} (Mgm^{-3})	2.453
μ (mm^{-1})	31.065
F (000)	788.0
2θ (°)	19.026 to 133.186
Reflections measured	3782
Independent reflections	1983 [R_{int} = 0.0346, R_{sigma} = 0.0433]
S	1.064
Final R_1, wR_2 indices (obs.)	R_1 = 0.0456, wR_2 = 0.1188
R_1, wR_2 indices (all)	R_1 = 0.0525, wR_2 = 0.1250

$R_1 = (\Sigma||F_o| - |F_c|| / \Sigma |F_o|)$. $wR_2 = [\Sigma (w(F_o^2 - F_c^2)^2) / \Sigma (w |F_o^2|^2)]^{1/2}$

Table S2. Selected bond distances (Å) and bond angles (º) of Tb-NDBC.

bond distances	
Tb1-Tb1[1]=3.9549(7)	Tb1-O1=2.456(5)
Tb1-O11=2.304(5)	Tb1-O1[4]=2.572(5)
Tb1-O12[1]=2.325(6)	Tb1-O2[5]=2.371(5)

Tb1-O13[2]=2.316(5)	Tb1-O2[4]=2.568(5)
Tb1-O14[3]=2.260(5)	
bond angles	
O11-Tb1-Tb1[1]=67.10(13)	O11-Tb1-O12[1]=136.15(19)
O11-Tb1-O13[2]=76.77(19)	O11-Tb1-O1[3]=82.20(19)
O11-Tb1-O1=152.11(18)	O11-Tb1-O2[4]=72.06(19)
O11-Tb1-O2[3]=71.64(19)	O12[1]-Tb1-Tb1[1]=69.10(13)
O12[1]-Tb1-O1[3]=92.2(2)	O12[1]-Tb1-O1=70.69(18)
O12[1]-Tb1-O2[4]=75.3(2)	O12[1]-Tb1-O2[3]=71.6(2)
O13[2]-Tb1-Tb1[1]=142.45(14)	O13[2]-Tb1-O12[1]=145.22(19)
O13[2]-Tb1-O1[3]=80.14(18)	O13[2]-Tb1-O1=75.46(19)
O13[2]-Tb1-O2[3]=123.30(19)	O13[2]-Tb1-O2[4]=136.71(19)
O14[5]-Tb1-Tb1[1]=117.18(13)	O14[5]-Tb1-O11=101.14(19)
O14[5]-Tb1-O12[1]=100.2(2)	O14[5]-Tb1-O13[2]=78.74(19)
O14[5]-Tb1-O1[3]=157.20(17)	O14[5]-Tb1-O1=75.98(18)
O14[5]-Tb1-O2[3]=152.28(17)	O14[5]-Tb1-O2[4]=78.64(18)
O1[3]-Tb1-Tb1[1]-85.06(11)	O1-Tb1-Tb1[1]=139.30(13)
O1-Tb1-O1[3]-90.48(10)	O1[3]-Tb1-O2[3]-50.23(17)
O1-Tb1-O2[3]=122.92(17)	O2[3]-Tb1-Tb1[1]=35.12(12)
O2[4]-Tb1-Tb1[1]=38.54(13)	O24-Tb1-C13=98.24(19)
O24-Tb1-O13=123.31(17)	O24-Tb1-O1=132.52(18)
O24-Tb1-O23=73.7(2)	

Symmetry codes for bond distances: [1] 1-*x*, 1-*y*, -*z*; [2] -*x*, 1/2+*y*, -1/2-*z*; [3] -*x*, 1-*y*, -*z*; [4] *x*, 3/2-*y*, -1/2+*z*; [5] 1-*x*, -1/2+*y*, 1/2-*z*; For bond angles: 1-*x*, 1-*y*, -*z*; [2] -*x*, 1/2+*y*, -1/2-*z*; [3] *x*, 3/2-*y*, -1/2+*z*; [4] 1-*x*, -1/2+*y*, 1/2-*z*; [5] -*x*, 1-*y*, -*z*; [6] -*x*, -1/2+*y*, -1/2-*z*; [7] *x*, 3/2-*y*, 1/2+*z*; [8] 1-*x*, 1/2+*y*, 1/2-*z*.

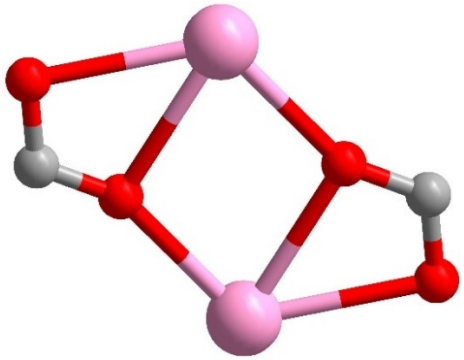

Fig. S1. The structural motif of $Tb_2(COO)_2$ subunit.

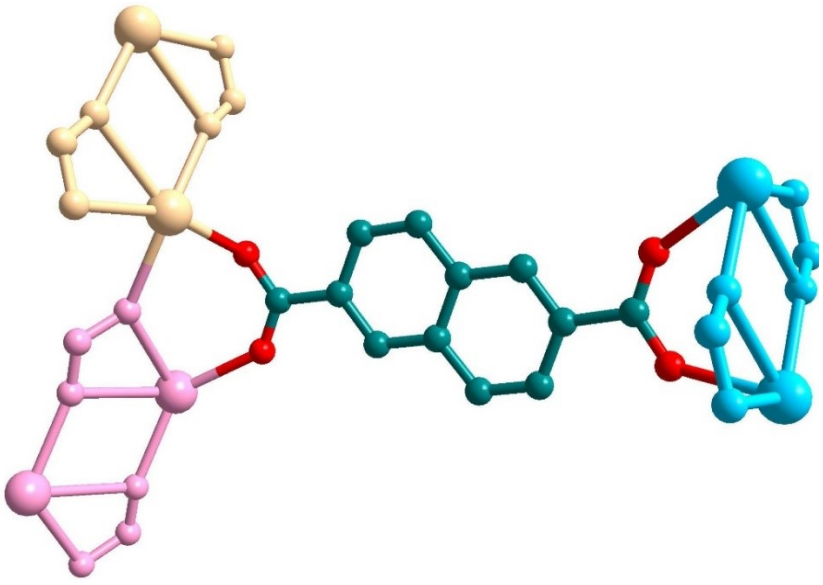

Fig. S2. The linkage mode of $NDBC^{2-}$ ligand with three $Tb_2(COO)_2$ subunits.

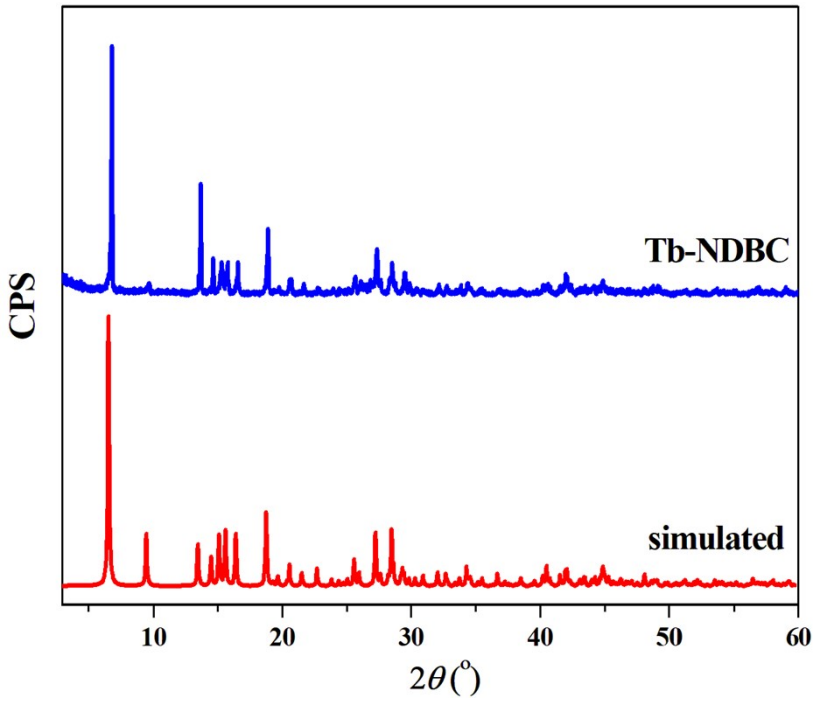

Fig. S3. Experimental PXRD pattern of Tb-NDBC compared to the simulated one.

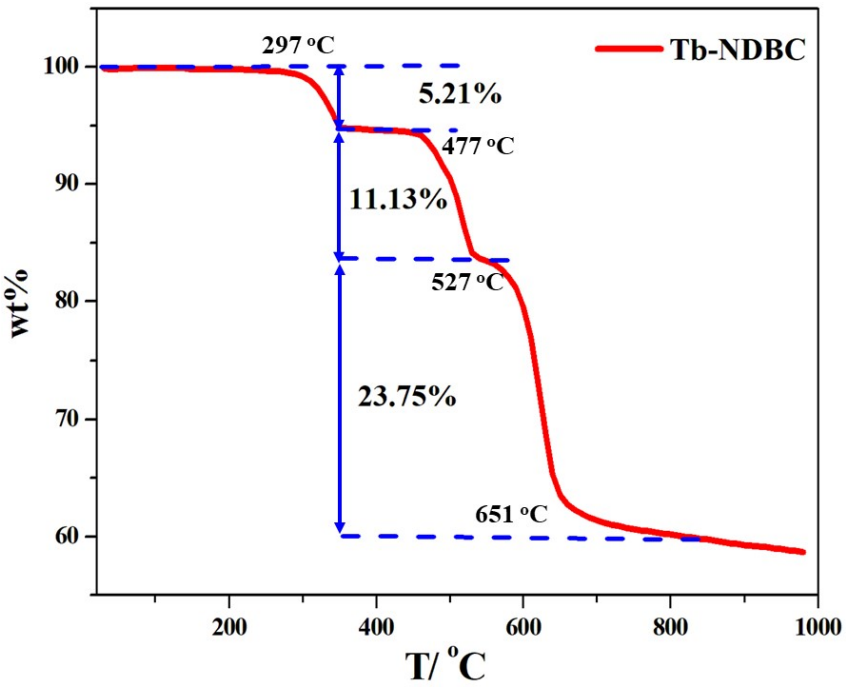

Fig. S4. The TG curve of Tb-NDBC.

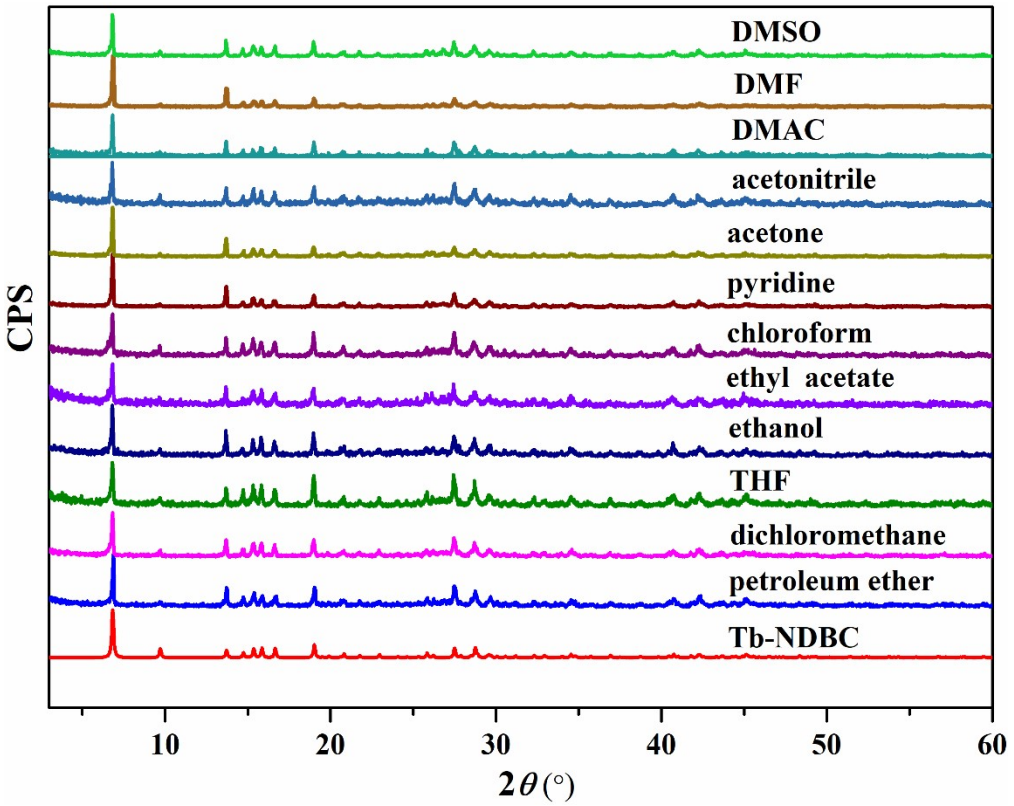

Fig. S5. Experimental PXRD patterns of Tb-NDBC immersed in twelve organic solvents for 48 h compared to the one of Tb-NDBC.

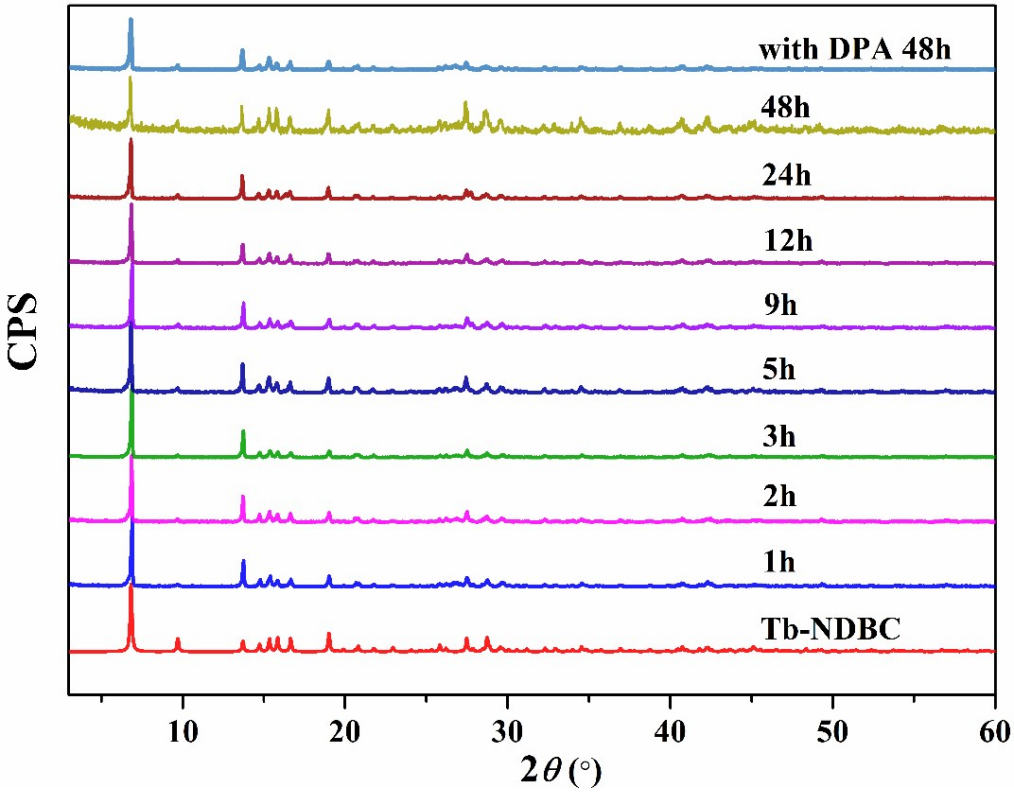

Fig. S6. Experimental PXRD patterns of Tb-NDBC immersed in water for 1-48 h compared to the one of Tb-NDBC.

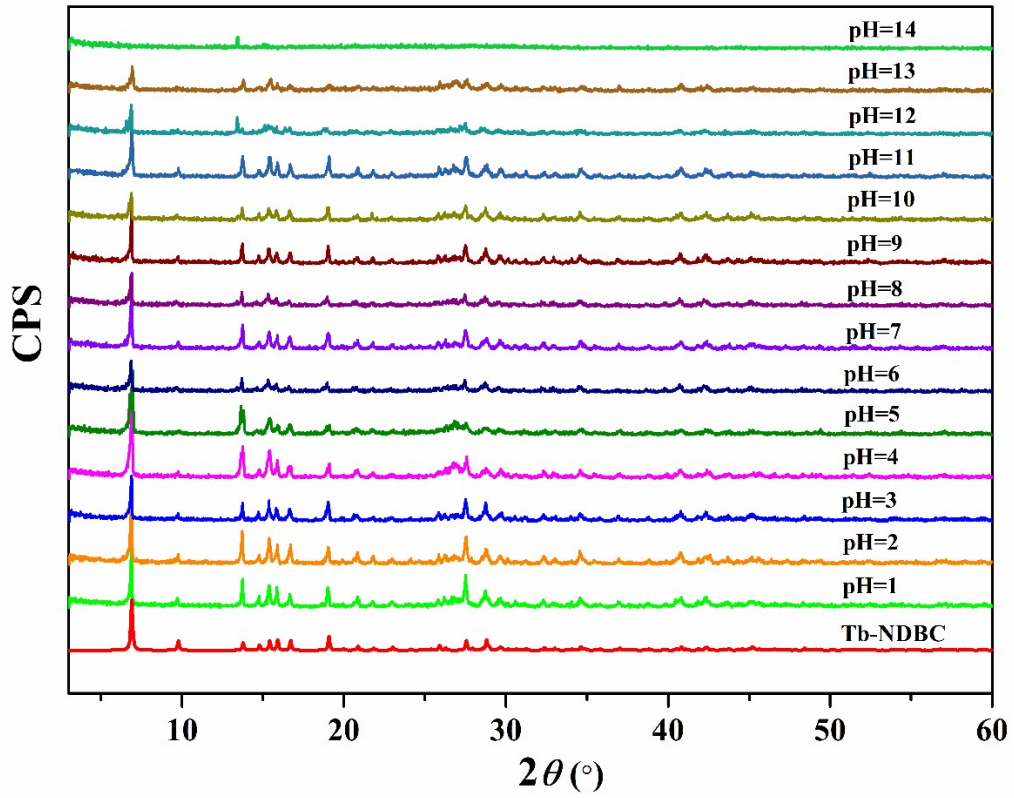

Fig. S7. Experimental PXRD patterns of Tb-NDBC immersed in HCl or NaOH aqueous solutions for 48h with pH =1-14 compared to the one of Tb-NDBC.

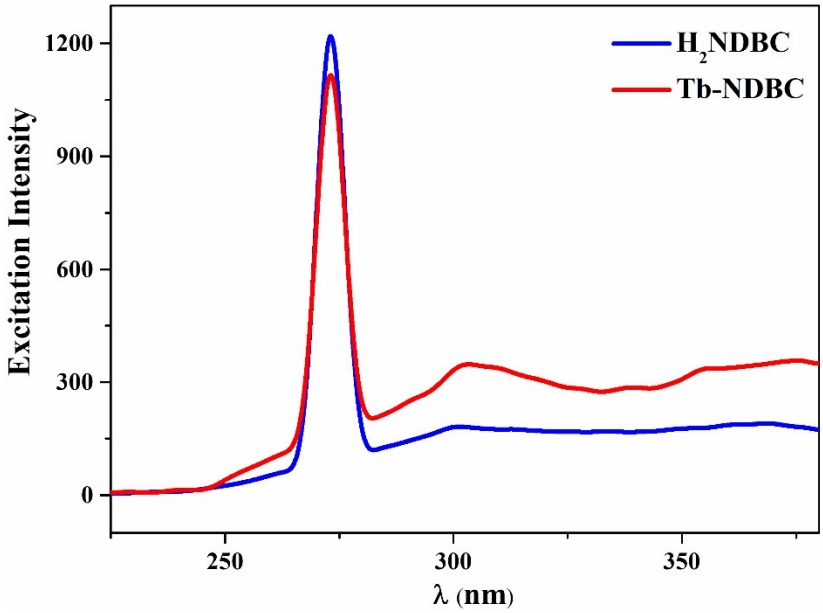

Fig. S8. Excitation spectra of Tb-NDBC and H_2NDBC recorded at ambient temperature.

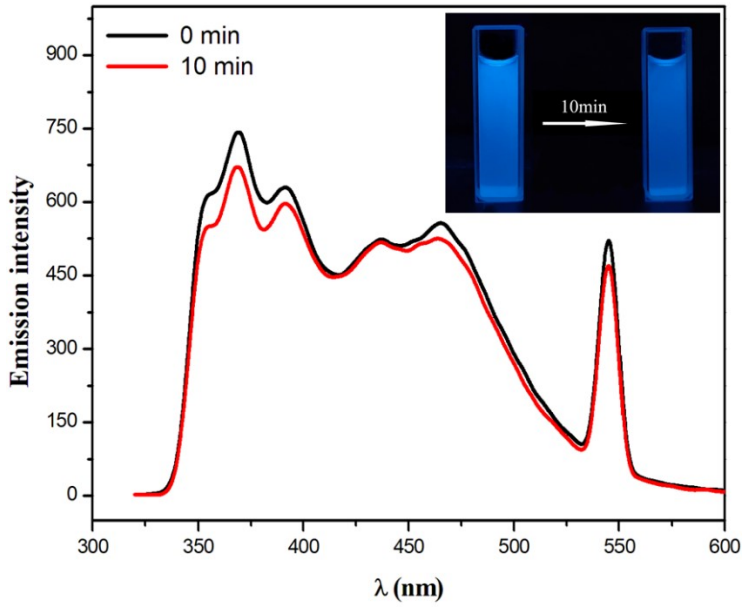

Fig. S9. Emission spectra of Tb-NDBC suspension with standing for 0 and 10min (inset: photo of cuvette taken under 365 nm UV light).

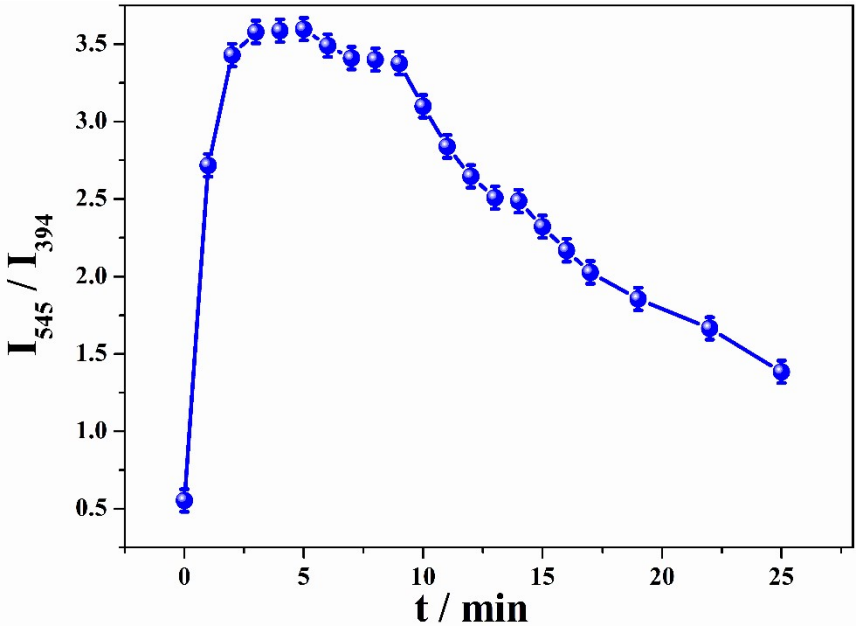

Fig. S10. The plot of I_{545}/I_{394} vs time of Tb-NDBC suspensions mixed with DPA with time ranging 0-25 min.

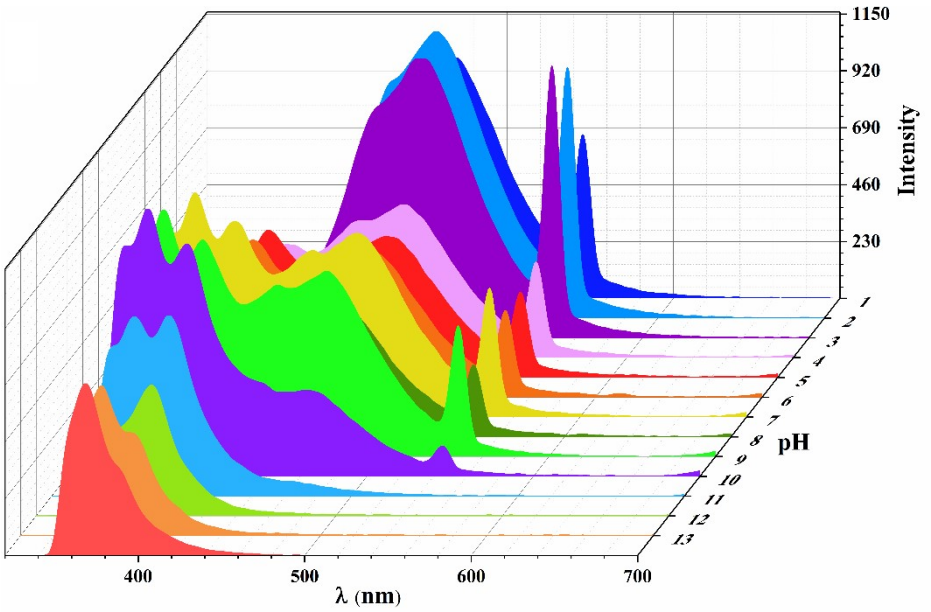

Fig. S11. The emission spectra of Tb-NDBC suspensions excited at 270 nm with pH ranging 1-14 without DPA added at ambient temperature.

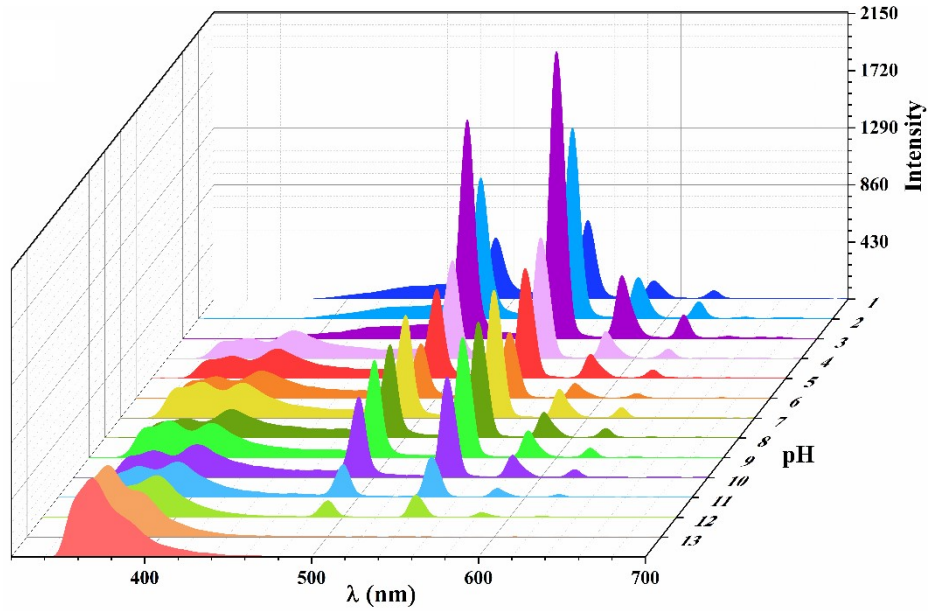

Fig. S12. The emission spectra of Tb-NDBC suspensions excited at 270 nm with pH ranging 1-14 with DPA added at ambient temperature.

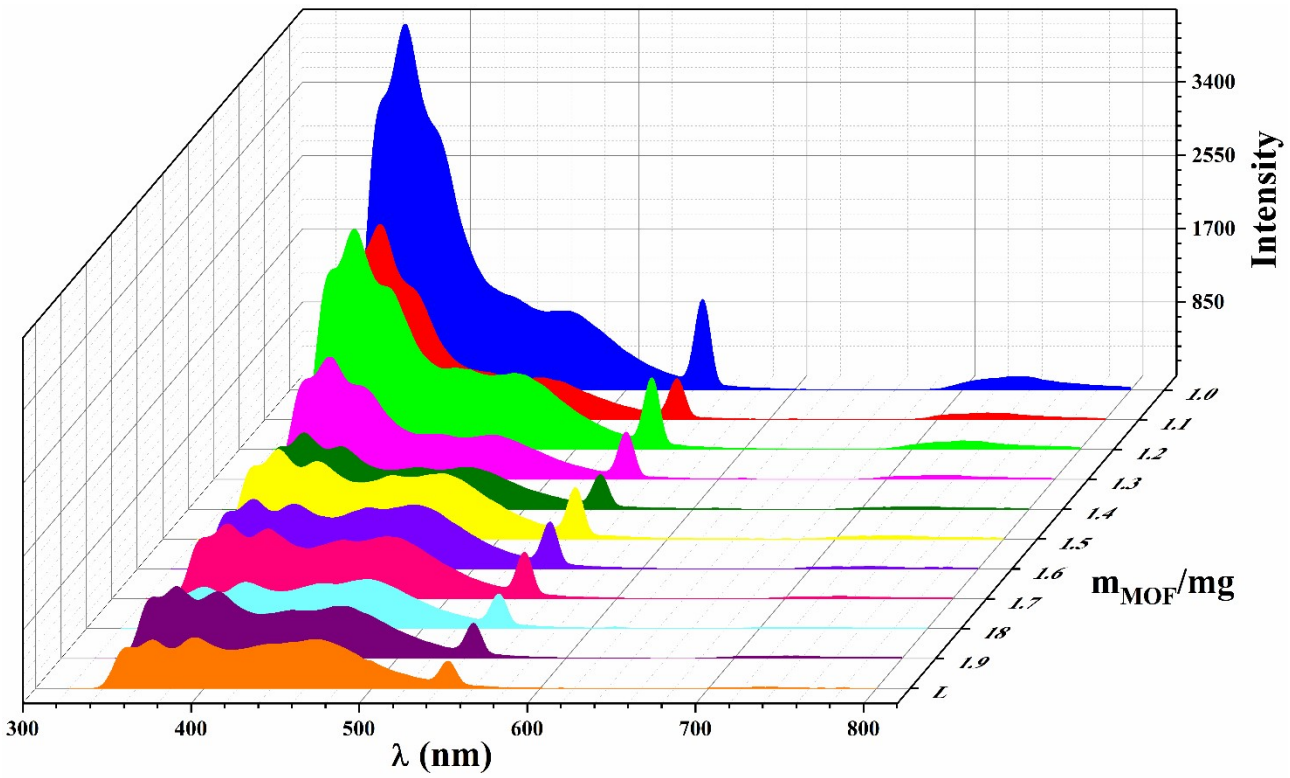

Fig. S13. The emission spectra of Tb-NDBC suspensions excited at 270 nm depending on the dosage of Tb-NDBC in 1-2 mg without DPA added at ambient temperature.

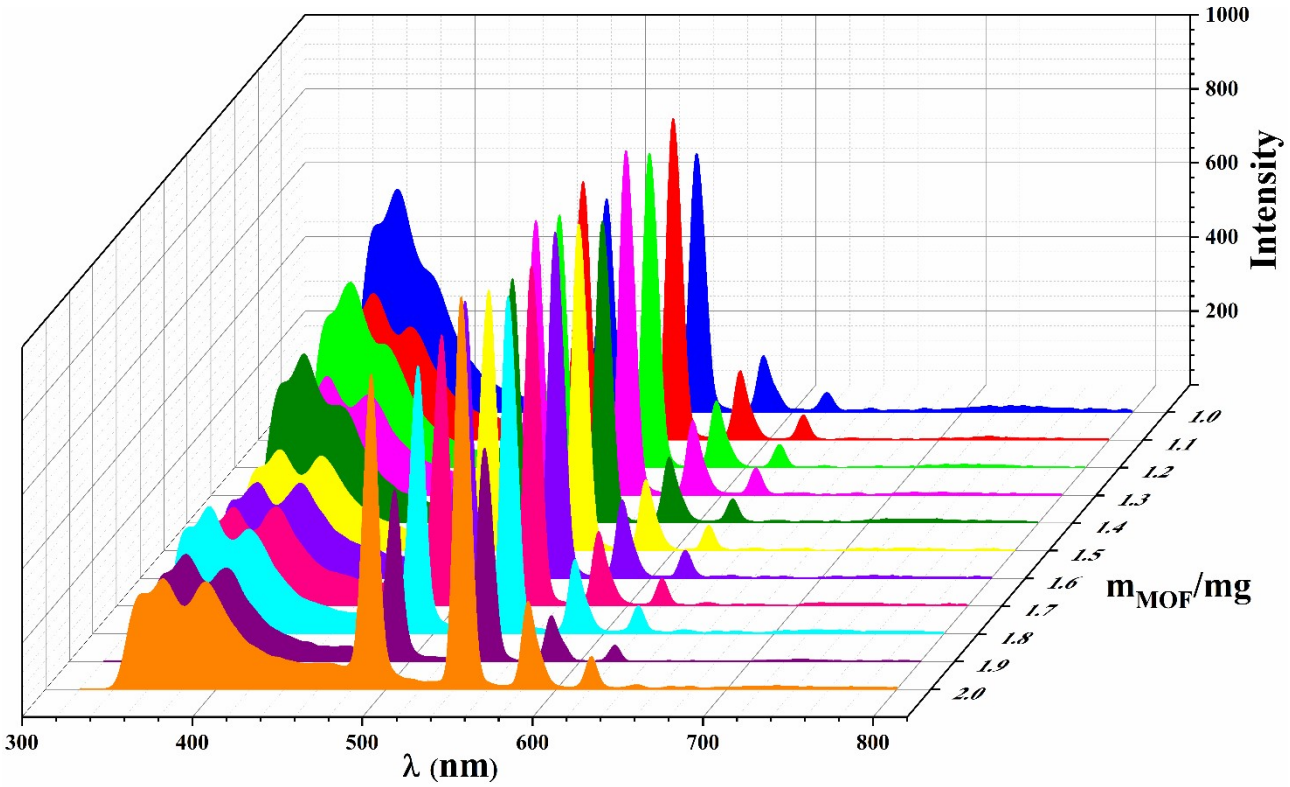

Fig. S14. The emission spectra of Tb-NDBC suspensions excited at 270 nm depending on the dosage of Tb-NDBC in 1-2 mg with DPA added at ambient temperature.

Table S3. Ten data of I_{545}/I_{394} for the blank sample

No.	1	2	3	4	5	6	7	8	9	10	SD (n=10)
I_{394}	621.1	549.5	556.8	559.8	569.2	568.5	578.7	757.3	585.4	589	
I_{545}	520.3	453.6	456.8	461.7	464.5	463.5	469.9	612.9	467	469	
I_{545}/I_{394}	0.838	0.825	0.820	0.825	0.816	0.815	0.812	0.809	0.798	0.796	0.01264

Table S4. Detection performance comparison of sensors to DPA detection

Sensors	Methods	Linear ranges	LODs	Refs
Tb-NDBC	Fluorometric	0-400μm	5.21μM	This work
$Tb_{0.875}Eu_{0.125}$-Hddb	Fluorometric	0-100μM	0.8494μM	1
$Eu_{0.1}Tb_{0.9}(NDBC)(H_2O)Cl$	Fluorometric	0-600 μM	0.248 μM	2
$Eu_{0.1}Tb_{0.9}(BPDC)(H_2O)Cl$	Fluorometric	0-400 μM	0.874 μM	2
$Eu_{0.1}Tb_{0.9}(BDC)(H_2O)Cl$	Fluorometric	0-300 μM	2.277 μM	2
Eu/Tb(BTC)	Fluorometric	0-1000 nM	1.087 μM	3
$[Tb_{0.43}Eu_{1.57}(1,4\text{-phda})_3(H_2O)](H_2O)_2$	Fluorometric	0-800 nM	0.17 μM	4
NH_2-MOF-76(Eu);	Fluorometric	0–100 μM	3.8 μM	5
Tb^{3+}/Eu^{3+}@Ni-BTC	Fluorometric	0-20μM	14.7 nM	6
RSPh@EuBTC	Colorimetric, Fluorometric	0-140 μM	2.2 μM	7
1-Cu^{2+}	Fluorometric, Colorimetric	0-10nm	2μM	8
EDTA-Eu^{3+}	Fluorometric	10-50nm	10nM	9
GMP-Tb/Eu	Fluorometric	2-16μM	96 nM	10
His@ZIF-8/Tb^{3+}	Fluorometric	0.08-10μM	0.02μM	11
TPE-TS@Eu/GMP ICP	Colorimetric	0-40μM	30, 27nm	12
Pal@FL@UiO-66-$(COOH)_2$-Eu	Fluorometric	0-35μM	9.3 nM	13
TbP-CPs	Fluorometric	0-8.0μM	54nM	14
Tb-COP	Fluorometric	0.1-30μM	13.5 nM	15
R6H@Eu(BTC)	Fluorometric	0-80μM	4.5 μM	16
Atta-RhB@SiO_2-EDTA-Tb	Fluorometric	0.1-40μM	9.8 nM	17
RiP/Eu^{3+} CPs	Fluorometric	0-1μM	41.5 nM	18
EBT-Eu^{3+}	Fluorometric Colorimetric	2-10μM	2 μM	19
Tb^{3+}@UIO-67	Fluorometric	0.3-6μM	36 nM	20
UCNPs-TPP/EBT	Colorimetric	2-200μM	0.9μM	21
Eu@SiNPs	Fluorometric	4-20μM	0.15 μM	22
pSiNPs-Tb	Fluorometric	1-10μM	1.25 μM	23
Fe_3O_4-Tb NP	Fluorometric	20-1000nM	5.4 nM	24
HAP-NPs	Fluorometric	0.1-40μM	77 nM	25
AuNPs	SERS	0.5-4μM	5 fM	26
Si NPs/Tb-MOFs	Fluorometric	0.025-3μM	5.3 nM	27
CD-Cu(II)	Fluorometric	0.25-20μM	12 nM	28
CdS@ZIF-8	Fluorometric	0.1-150μM	67 nM	29
CDs-Tb	Fluorometric	0.0005-2.5μM	0.1 nM	30
OG-CDs	Fluorometric	0.5-12.5μM	56 nM	31
Eu-CDs	Fluorometric	5-700nM	5nM	32
FMn-CDs	Fluorometric	0.1-750nM	0.1 nM	33
CDs-Eu	Fluorometric	0.5nM-5μM	0.8 nM	34
hPEI-CD-EDTA-Eu^{3+}	Fluorometric	1.0-100nM,	190 pM	35
EBT-CDs@Eu	Fluorometric	0.1-12.0μM	10.64 nM	36
CdS QDs -Eu^{3+}	Fluorometric	1-120μM	0.2 μM	37
BCNO QDs-EDTA-Eu^{3+}	Fluorometric	0-700nM	0.5 nM	38
SiQDs-NH_2-EDTA-Eu	Fluorometric	0-34μM	1.02 μM	39
Au@GSH NC-Cu^{2+}	Fluorometric	1-4μM	19nM	40
Sm^{3+}/Au(0)@Au(I)-SG NCs	Fluorometric	1-120μM	0.1 μM	41
BSA-Au NCs	Fluorometric	0-66.7μM	35.8 nM	42

Note: H_4ddb=1,3-di(3',5'-dicarboxylphenyl)benzene; $BPDC^{2-}$=4,4'-biphenyldicarboxylate; BDC^{2-}=1,4-benzenedicarboxylate; BTC^{3-}= 1,3,5-benzenetricarboxylate;1,4-phda=1,4-phenylenediacetic acid; 1=atechol-substituted monostyryl boradiazaindacene probe; EDTA=ethylenediaminetetraacetic acid dianhydride; GMP=guanine 5′-monophosphate; R6H=rhodamine-based sensing probe; monophosphate; His=L-histidine; ZIF=zeolitic imidazolate framework; TPE-TS=tetra(4-sulfophenyl)ethylene; ICP=Infifinite

coordination polymer; Pal@FL=Pal-doped fluorescein; RSPh=rhodamine; TbP=terbium; CPs=coordination polymer microspheres; COP=covalent organic polymer; Atta=attapulgite; RhB= Rhodamine B; RiP = riboflflavin-50-phosphate; EBT=eriochrome Black T; UCNPs=upconversion nanoparticles; TPP=tripolyphosphate; pSiNPs=porous silicon nanoparticles; HAP=hydroxyapatite; CD=carbon dot; OG=orange/green dual-emissive; FMn=functionalized manganese-doped; hPEI=hyperbranched polyethyleneimine; QDs= quantum dots; BCNO =boron carbon oxynitride; GSH=glutathione; NCs=nanoclusters; SG =glutathione; BSA=bovine serum albumin; phosphonate.

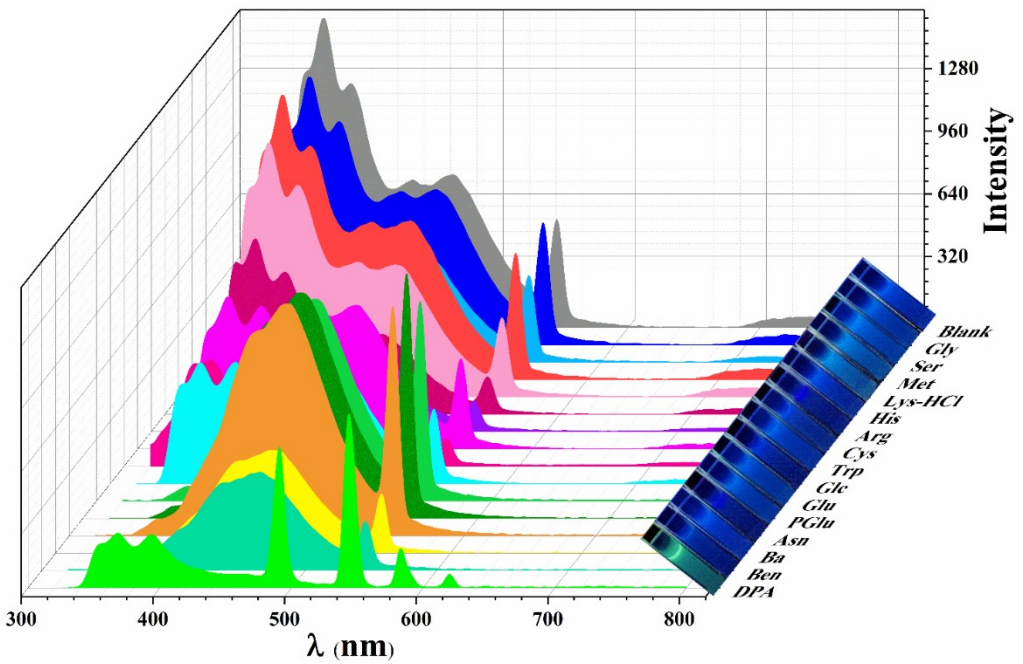

Fig. S15. The emission spectra of 1.8 mg Tb-NDBC suspensions excited at 270 nm with fourteen kinds of 1 mM interferents with photos taken under 365 nm UV light.

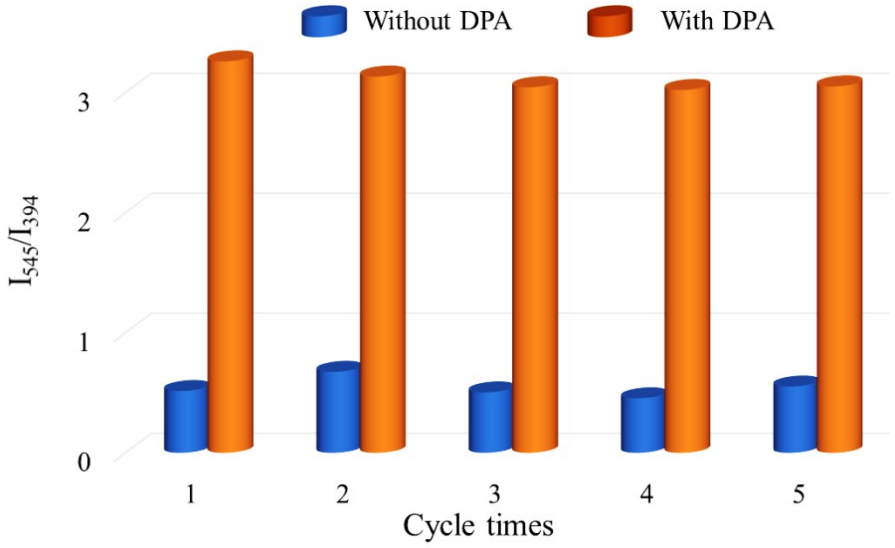

Fig. 16. The durability of Tb-NDBC in five DPA detections.

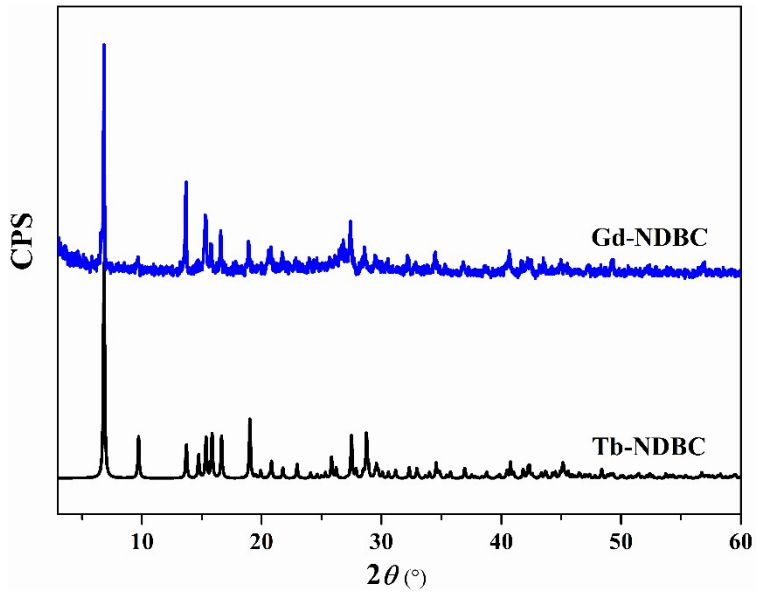

Fig. S17. The PXRD pattern of Gd-NDBC comparing to Tb-NDBC.

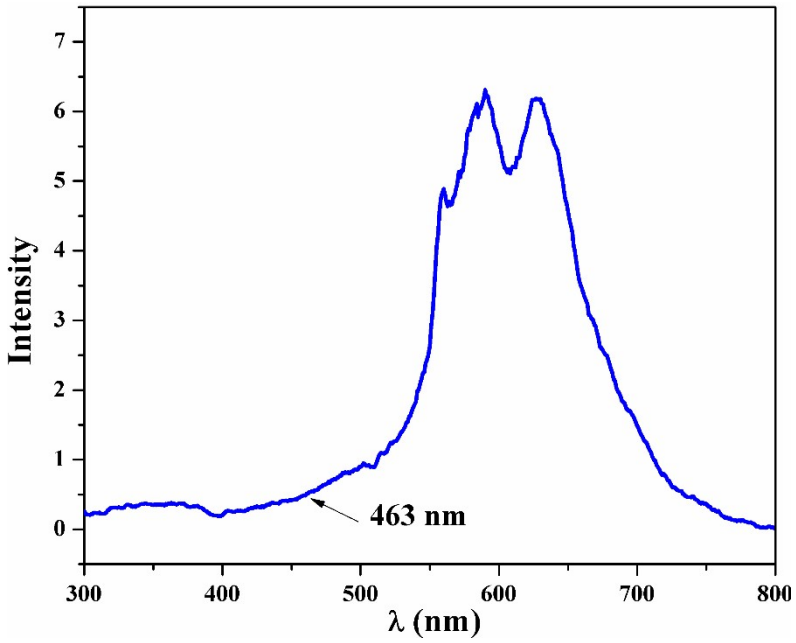

Fig. S18. Phosphorescence spectrum of Gd-NDBC under 340 nm excitation at 77K.

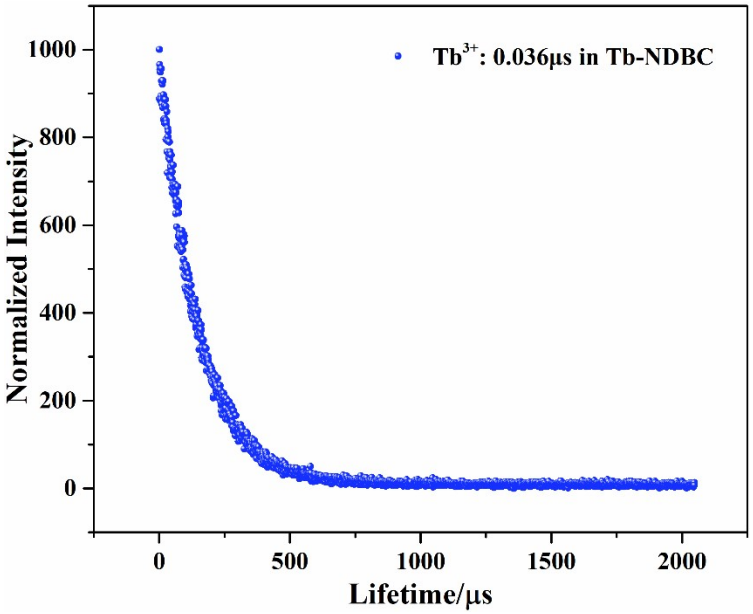

Fig. S19. The fluorescence lifetime of Tb^{3+} in Tb-NDC without DPA.

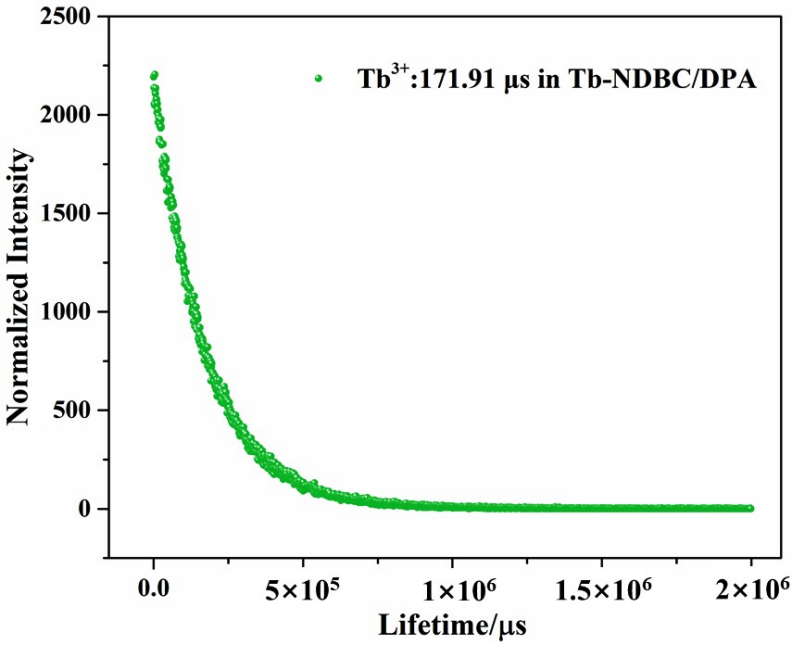

Fig. S20. The fluorescence lifetime of Tb^{3+} in Tb-NDC with DPA.

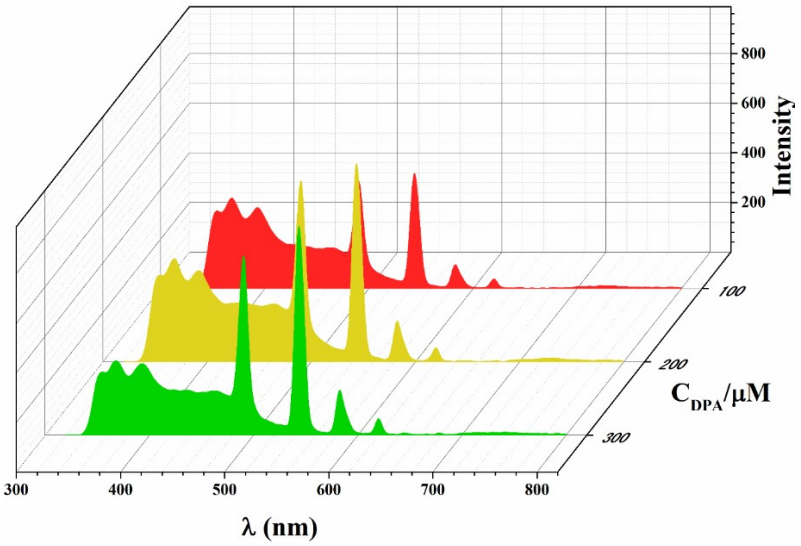

Fig. 21. The emission spectra of Tb-NDBC suspensions in human serum with C_{DPA} = 100, 200 and 300 μM excited at 270 nm at ambient temperature.

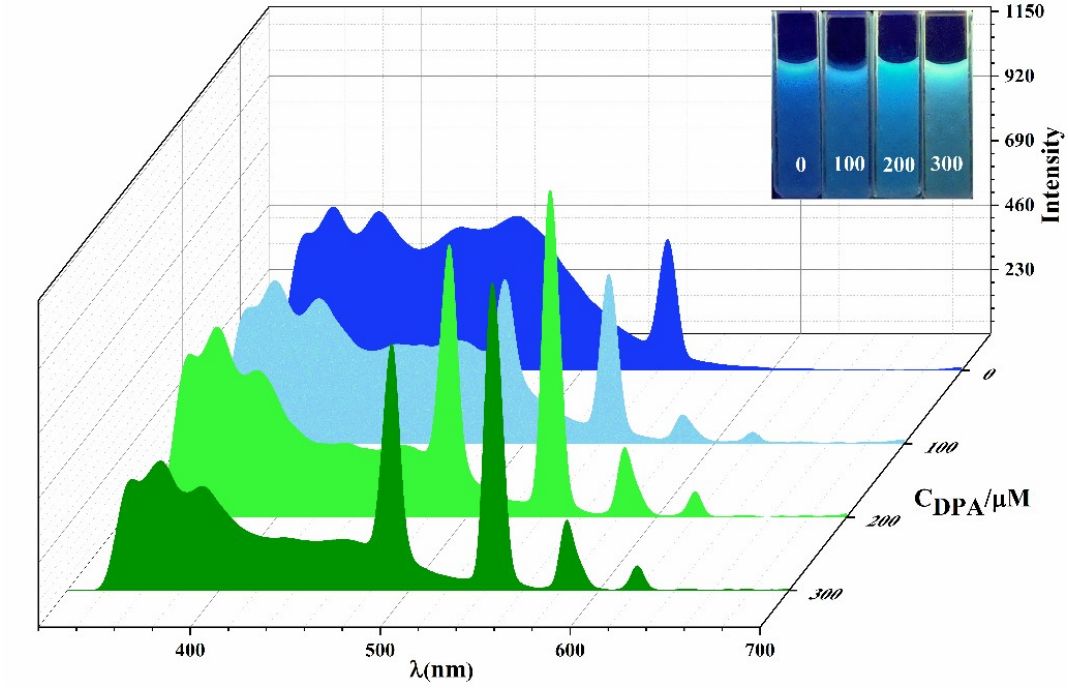

Fig. 22. The emission spectra of Tb-NDBC suspensions in lake water with C_{DPA} = 100, 200 and 300 μM excited at 270 nm at ambient temperature with photos taken under 365 nm UV light.

1. X. B. Chen, C. X. Qi, Y. B. Xu, H. Li, L. Xu and B. Liu, *J. Mater. Chem. C*, 2020, **8**, 17325.
2. M. L. Shen, B. Liu, L. Xu and H. Jiao, *J. Mater. Chem. C*, 2020, **8**, 4392.
3. M. N. Wu, Y. X. Zhuang, J. B. Liu, W. W. Chen, X. Y. Li and R. J. Xie, *Opt. Mater.*, 2020, **106**, 110006.
4. J. Othong, J. Boonmak, F. Kielar, S. Hadsadee, S. Jungsuttiwong and S. Youngme, *Sensor. Actuat B-Chem.*, 2020, **316**, 128156.
5. D. Wu, Z. Zhang, X. W. Chen, L. K. Meng, C. G. Li, G. H. Li, X. B. Chen, Z. Shi and S. H. Feng, *Chem. Commun.*, 2019, **55**, 14918.
6. H. Lei, C. X. Qi, X. B. Chen, T. Zhang, L. Xu and B. Liu, *New J. Chem.*, 2019, **43**, 18259.

7. X. M. Li, J. Y. Zhao, Y. Y. Zhu, B. L. Wang, X. F. Wei, Y. Y. Shao, Y. S. Ma and T. Y. Jiang, *Spectrochim. ACTA A*., 2020, **229**, 117999.
8. Y. Cetinkaya, M.N.Z. Yurt, H. Avni Oktem and M.D. Yilmaz, *J. Hazard. Mater.*, 2019, **377**, 299.
9. M. Donmez, H.A. Oktem and M.D. Yilmaz, *Carbohydr. Polym*., 2018, **180**, 226
10. N. Gao, Y. F. Zhang, P. C. Huang, Z. H. Xiang, F. Y. Wu and L. Q. Mao, *Anal. Chem*., 2018, **90**, 7004.
11. L. Guo, M. Liang, X. Wang, R. Kong, G. Chen, L. Xia and F. Qu, *Chem. Sci.*, 2020, **11**, 2407.
12. C. Huang, R. Ma, Y. Luo, G. Shi, J. Deng and T. Zhou, *Anal. Chem.*, 2020, **92**, 12934.
13. L. Jia, X. Chen, J. Xu, L. Zhang, S. Guo, N. Bi and T. Zhu, *J. Hazard. Mater.*, 221, **402**, 123776.
14. Y. Luo, L. Zhang, L. Zhang, B. Yu, Y. Wang and W. Zhang, *ACS Appl. Mater. Interfaces*, 2019, **11**, 15998.
15. S. Qu, N. Song, G. Xu and Q. Jia, *Sensors Actuat. B-Chem*., 2019, **290**, 9.
16. J. B. Dunn, M. L. Burns, S. E. hunter and P. E. Savage, *J. Supercrit. Fluid*., 2003, **27**, 263.
17. J. Xu, X. Shen, L. Jia, C. Zhang, T. Ma, T. Zhou, T. Zhu, Z. Xu, J. Cao, B. Liu, N. Bi, L. Liu and Y. Li, *Dyes Pigments*, 2018, **148**, 44.
18. S. F. Xue, J. F. Zhang, Z. H. Chen, X. Y. Han, M. Zhang and G. Shi, *Anal. Chim. Acta*, 2018, **1012**, 74.
19. M. D. Yilmaz and H.A. Oktem, *Anal. Chem*., 2018, **90**, 4221.
20. X. Zhang, W. Zhang, G. Li, Q. Liu, Y. Xu and X. Liu, *Mikrochim. Acta*, 2020, **187**, 122.
21. Z. H. Cheng, X. Liu, S. Q. Zhang, T. Yang, M. L. Chen and J. H. Wang, *Anal. Chem*., 2019, **91**,12094
22. M. Na, S. Zhang, J. Liu, S. Ma, Y. Han, Y. Wang, Y. He, H. Chen and X. Chen, *J. Hazard. Mater*., 2020, **386**, 121956.
23. Y. Jung, S. Kang, J. An, J. Jung and D. Kim, *Dyes Pigments*, 2020, **182**, 108700.
24. T. M. Koo, M. J. Ko, B. C. Park, M. S. Kim and Y. K. Kim, *J. Hazard. Mater.*, 2021, **408**, 124870.
25. Y. Li, X. Li, D. Wang, C. Shen and M. Yang, *Mikrochim. Acta*, 2018, **185**, 435.
26. T. K. Naqvi, A. Bajpai, M. S. S. Bharati, M. M. Kulkarni, A. M. Siddiqui, V. R. Soma, P. K. Dwivedi, *J. Hazard. Mater*., 2021, **407**, 124353.
27. D. Yang, S. Mei, Z. Wen, X. Wei, Z. Cui, B. Yang, C. Wei, Y. Qiu, M. Li, H. Li, W. Zhang, F. Xie, L. Wang and R. Guo, *Mikrochim. Acta*, 2020, **187**, 666.
28. P. Li, A. N. Ang, H. Feng and S. F. Y. Li, J. Mater. Chem. C, 2017, 5, 6962
29. X. Li, J. Luo, L. Deng, F. Ma and M. Yang, *Anal. Chem*., 2020, **92**, 7114.
30. M. L. Liu, B. B. Chen, J. H. He, C. M. Li, Y. F. Li and C. Z. Huang, *Talanta*, 2019, **191**, 443.
31. L. F. Pang, H. Wu, M. X. Wei, X. F. Guo and H. Wang, *Spectrochim. Acta A Mol. Biomol. Spectrosc.*, 2021, **244**, 118872.
32. M. Rong, X. Deng, S. Chi, L. Huang, Y. Zhou, Y. Shen and X. Chen, *Mikrochim. Acta*, 2018, **185**, 201.
33. M. Rong, Y. Liang, D. Zhao, B. Chen, C. Pan, X. Deng, Y. Chen and J. He, *Sensors Actuat. B-Chem*., 2018, **265**, 498.
34. J. Wang, D. Li, Y. Qiu, X. Liu, L. Huang, H. Wen and J. Hu, *Talanta*, 2020, **220**, 121377.
35. H. Yang, F. Lu, X. Zhan, M. Tian, Z. Yuan and C. Lu, *Talanta*, 2020, **208**, 120368.
36. Q. Zhou, Y. Fang, J. Li, D. Hong, P. Zhu, S. Chen, K. Tan, *Talanta*, 2021, **222**, 121548.
37. X. Li, L. Deng, F. Ma and M. Yang, *Mikrochim. Acta*, 2020, **187**, 287.
38. M. Rong, X. Yang, L. Huang, S. Chi, Y. Zhou, Y. Shen, B. Chen, X. Deng and Z. Q. Liu, *ACS Appl. Mater. Interfaces*, 2019, **11**, 2336.
39. Z. Zhou, J. Gu, Y. Chen, X. Zhang, H. Wu and X. Qiao, *Spectrochim. Acta A Mol. Biomol. Spectrosc*., 2019, **212**, 88.
40. M. M. F. Baig and Y. C. Chen, *Analyst*, 2019, **144**, 3289.
41. M. I. Halawa, B. S. Li and G. Xu, *ACS Appl. Mater. Interfaces*, 2020, **12**, 32888.

42. X. Liu, Y. Qiu, B. Li, Z. Li, Y. Zhang, J. Wang and Q. Xiong, *Spectrochim. Acta A Mol. Biomol. Spectrosc.*, 2020, **240**, 118541.